Compact Microstrip Resonators for 900 MHz Frequency Band

M. G. Banciu, R. Ramer, and A. Ioachim

***Abstract*—A technique to reduce the size of planar resonators is investigated using a transmission line model and a finite-difference time-domain (FDTD) method. New miniaturized square microstrip resonators are proposed for 900 MHz band. The resonators offer low impedance sections leading to a better handling of power. The feasibility of compact filters using the proposed resonators is demonstrated. The input/output coupling lines of a two-pole filter have been positioned in a way that produces a filter response with transmission zeros on the both sides of the pass-band. Sharper skirts and higher out-of-band rejection are obtained for four-pole filters with cross-coupled resonators.**

***Index Terms*—Cross-coupled resonators, microstrip filters, stepped-impedance resonators, wireless passive components.**

I. Introduction

RAPID evolution of the mobile communications systems requires miniaturized low-cost RF components with improved performance. Simple squared open-loop resonators have been proposed for low-cost microstrip filters [1]. Nevertheless, for low frequency bands, such as the 900 MHz band of the General Packet Radio Service (GPRS), the size reduction requires even more compact resonators and filters.

The newly proposed type of microstrip resonators were designed in a square shape due to its versatility in offering several inter-resonator coupling options to the filter design. Designed for the same resonance frequency, the newly proposed 900 MHz resonators of types labeled **A**, **B**, **C**, **D** and **E**, are illustrated in Fig. 1(a)–(e). They are more compact than the square hairpin and the simple half-wavelength loop resonators, which are shown in Fig. 1(g) and (h) respectively.

A miniaturized hairpin resonator in Fig. 1(f), with the same size as the resonators of types **C**, **D**, **E** will resonate at 986 MHz. Hence, its dimensions need to be increased for operation in the 900 MHz frequency band. Resonators of type **A** and **B** have a 10.64 mm edge compared to 9.52 mm edge for the resonators **C**, **D**, **E**. Thus, the first resonators cover 40% of the surface area of the simple loop half-wavelength resonator compared to the latter ones, which take up only 32%.

The resonators have been manufactured on Rogers substrate with 0.635 mm thickness and 10.8 ± 0.25 dielectric constant. The measured values of the unloaded quality factors Q_u are 152.5, 154, 120, 132.2 and 141.2 for type **A**, **B**, **C**, **D** and **E** resonators, respectively. These values are close to the quality factor $Q_u = 159$ of the simple hairpin resonator in Fig. 1(g), which occupies a larger area.

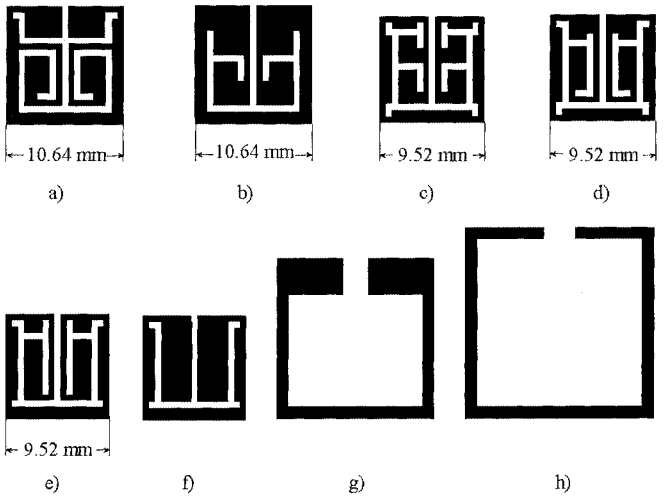

Fig. 1. Geometry of newly proposed resonators together with other microstrip resonators. (a) **A** type resonator, (b) **B** type resonator, (c) **C** type resonator, (d) **D** type resonator, (e) **E** type resonator, (f) miniaturized hair-pin resonator, (g) squared hair-pin resonator, and (h) half-wavelength loop resonator.

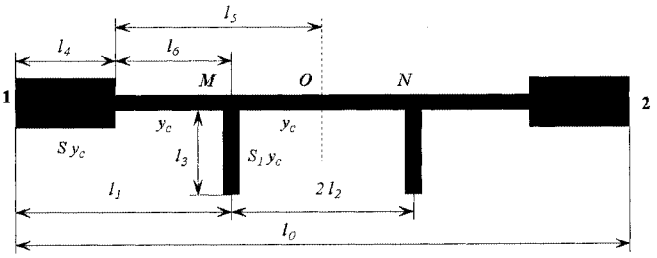

Fig. 2. Model of a stepped-impedance resonator with stubs added.

II. Transmission Line Model

A method of size reduction of planar resonators is proposed by investigating a stepped impedance resonator (SIR) with the admittance ratio S, $S > 1$, and the characteristic admittance y_c for the low admittance section. Two uniform stubs of characteristic admittance $S_1\,y_c$ are added symmetrically on both sides of point **O**, at points ***M*** and ***N*** as shown in Fig. 2. S_1 is the ratio of the stub admittance and the characteristic admittance y_c for the low admittance section of the stepped impedance resonator. The transmission lines are regarded as loss-less and nondispersive in this model. The same propagation constant β is considered for

Manuscript received December 4, 2002.

M. G. Banciu and R. Ramer are with the School of Electrical Engineering and Telecommunications, University of New South Wales, Sydney 2052 NSW, Australia (e-mail: GabrielBanciu@hotmail.com).

A. Ioachim is with the National Institute for Physics of Materials, Bucharest-Magurele, Romania.

Digital Object Identifier 10.1109/LMWC.2003.811673

1531-1309/03$17.00 © 2003 IEEE

all transmission line sections, with different characteristic impedances. The initial model does not take into account any discontinuities such as step-impedances, bends, open-end effects, junctions, etc.

The resonator size reduction while keeping the resonance frequency unchanged is equivalent to the decrease of the resonance frequency and having the size unchanged. It is already known [2] that the maximum reduction of resonance frequency, for a simple SIR without stubs, is obtained when the section with the high admittance $S\ y_c$ has the length equal to the half of the length of the section with low admittance y_c. Applying this condition to the SIR, illustrated in Fig. 2, leads to $l_4 = l_5$.

For the fundamental mode analysis, the symmetry point ***O*** in Fig. 2 may be considered as short-circuited. The resonance frequency f_0 of the fundamental mode is $f_0 = \beta_0/2\pi v_{eff}$, where v_{eff} is the effective propagation velocity along the line, and β_0 is the propagation constant at resonance. The cancellation of the input impedance at port ***1*** leads to the following equations in β:

$$[S_1 \tan(\beta l_3) - \cot(\beta l_2)][1 - S\tan(\beta l_4)\tan(\beta l_6)] + \tan(\beta l_6) + S\tan(\beta l_4) = 0, \text{ when } l_1 \geq l_4 \quad (1a)$$

and

$$[S + \cot(\beta l_5)\tan(\beta l_6)][S_1 \tan(\beta l_3) + S\tan(\beta l_1)] + S[S\tan(\beta l_6) - \cot(\beta l_5)] = 0, \text{ when } l_1 < l_4. \quad (1b)$$

The case $l_1 > l_4$ corresponds to the stub connection to the SIR segment with lower y_c characteristic admittance in Fig. 2. In the case $l_1 < l_4$, the stub is connected to the SIR segment with higher $S_1\ y_c$ characteristic admittance. The solution β_0 of (1a) gives the resonance frequency f_0 of the fundamental mode. As shown in Fig. 3, the resonance frequency f_0 decreases with the increase of the stub length l_3 and increases with the increase of the distance l_1, which gives the stub position. Dimensions are normalized to λ_{0init}, which is the wavelength corresponding to the resonance frequency $f_0 = 900$ MHz in our case. The resonance frequency f_0 also decreases with the increase of S, the admittance ratio of the SIR. This is illustrated in Fig. 4.

The analysis of the first higher order resonating mode provides information about the filter spurious pass-band. For the first higher mode analysis, the symmetry point ***O*** can be considered as open-circuited. The frequency f_1 of the first spurious mode can be obtained from the solutions of the following equations:

$$[S_1 \tan(\beta l_3) + \tan(\beta l_2)][1 - S\tan(\beta l_4)\tan(\beta l_6)] + \tan(\beta l_6) + S\tan(\beta l_4) = 0, \text{ when } l_1 \geq l_4 \quad (2a)$$

and

$$[S - \tan(\beta l_5)\tan(\beta l_6)][S_1 \tan(\beta l_3) + S\tan(\beta l_1)] + S[S\tan(\beta l_6) + \tan(\beta l_5)] = 0, \text{ when } l_1 < l_4. \quad (2b)$$

The ratio f_1/f_0 between the spurious mode and the fundamental frequencies reaches its maximum when $l_1 = l_3 = \lambda_{0init}/4$.

The resonator design is a compromise between the conditions of minimizing f_0 and maximizing the ratio f_1/f_0. For practical

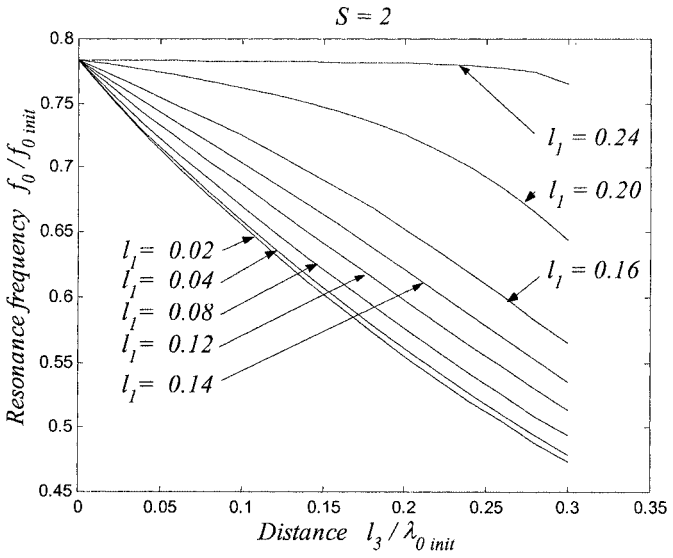

Fig. 3. Decrease of resonance frequency due to the stubs placed at various distances l_1, when $S = 2$. Dimensions are normalized to λ_{0init}.

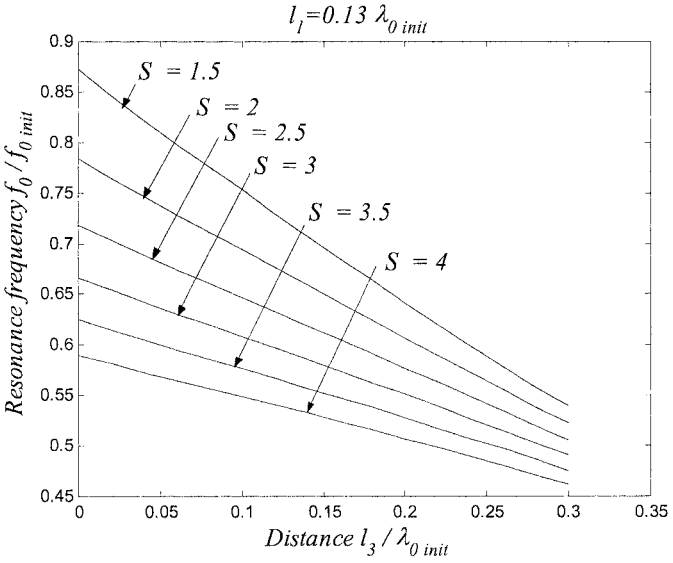

Fig. 4. The reduction in resonance frequency when the stubs position $l_1 = 0.13\lambda_{0init}$ is unchanged and S varies. Dimensions are normalized to λ_{0init}.

designs, illustrated in Fig. 1(a)–(e), a pair of nonuniform stubs are folded and added inside to the squared SIR. The type **A**, **C** and **E** resonators correspond to the case of $l_1 > l_4$, and the type **B** and **D** resonators correspond to the case $l_1 < l_4$. In the case of resonators of type **A**, **C**, **D** and **E**, the bend capacitance has been partially compensated. It was found that a higher degree of compactness could be obtained, when one pair rather than two pairs of nonuniform stubs was used [3]. In the design, only low-impedance transmission line sections with characteristic impedance $Z_c < 50\ \Omega$ were used. This attribute makes the proposed designs very attractive to HTS applications, where wide lines are strongly required for a better power handling [5]. The realization of newly proposed microstrip resonators and filters using these resonators is simple and does not require any via holes or additional lumped components.

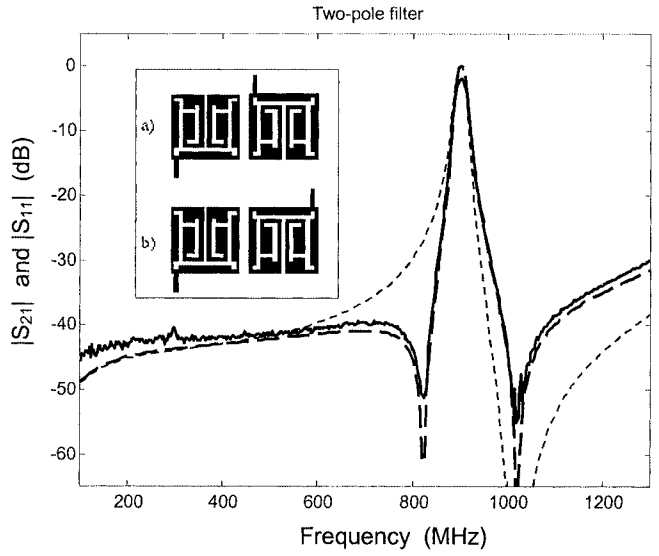

Fig. 5. Two-pole filter response using the **D** type resonators shown in Fig. 1(d). The solid line and the dashed line represent the measured and simulated response, respectively, for the structure shown in the (a) insert. The dotted line represents the simulated response of the filter shown in the insert (b).

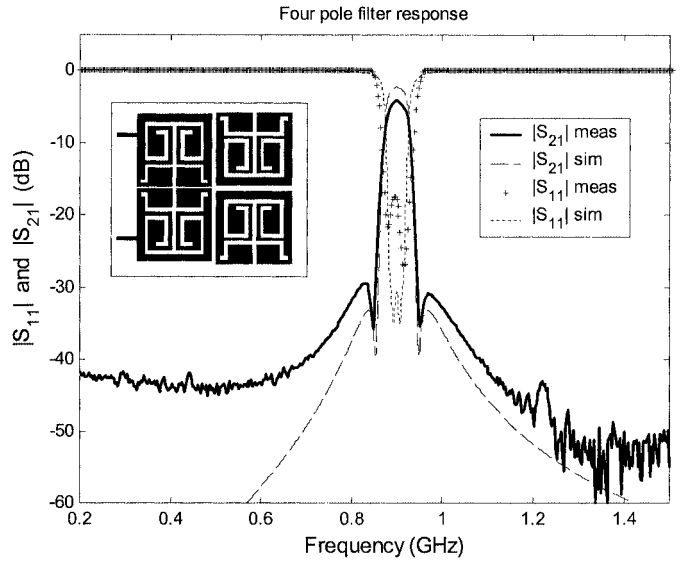

Fig. 6. Response of the four-pole filter using cross-coupled **A** type resonators shown in Fig. 1(a).

As the transmission line models are less accurate for the analysis of the final shape of resonators, a 3-D FDTD method was developed in-house. This method was used for the final microstrip resonator and filter design. The inter-resonator coupling coefficients and the external quality factors Q_e were also evaluated by employing the same in-house developed FDTD method. The total FDTD design time was considerably reduced as signal estimation and neural networks were included in the model [4].

III. Compact Microstrip Filters

Once the dependence of inter-resonators coupling coefficients on the resonators positions and spacing was calculated, we proceeded with the multi-pole filter design. Two-pole filters designed with **D** type resonators are shown in the insert of Fig. 5. For both (a) and (b) filter configurations, the coupling coefficient and the external quality factor are equal. Nevertheless, due to the asymmetric positions of the input/output coupling lines, the response of filter in configuration (a) exhibits two transmission zeros on both sides of the pass-band, compared to only one transmission zero for filter in configuration (b). The additional transmission null produces a sharp response at low frequencies.

An increased degree of control on the transmission nulls was achieved when designing a four-pole filter with cross-coupled **A** type resonators. The corresponding layout and filter response are shown in Fig. 6. The transmission zeros on both sides of the pass-band are due to the extra negative coupling between the first and fourth resonators (counted from the upper left clockwise). This confers a quasielliptic response [6] of the filter. The cross-coupling improves the filter skirt sharpness. The coupling matrix is

$$\mathbf{M}_4 = \begin{bmatrix} 0 & 0.0448 & 0 & -0.0074 \\ 0.0448 & 0 & 0.0356 & 0 \\ 0 & 0.0356 & 0 & 0.0448 \\ -0.0074 & 0 & 0.0448 & 0 \end{bmatrix}. \quad (3)$$

The external quality factor is $Q_e = 16.19$.

IV. Conclusions

The size of stepped impedance resonators can be reduced by addition of the stubs. The newly proposed resonators take up to 32% of the surface of a simple square half-wavelength resonator, both being designed for 900 MHz. Two-pole filters with transmission zeros on both sides of the pass-band were designed by using the miniaturized resonators. Four-pole more selective filters with improved out-of-band attenuation were obtained using cross-coupling configurations of the compact resonators. The filters realization does not require via holes or additional lumped components and makes them suitable for applications in wireless systems. The proposed designs are also attractive to HTS planar technology because the resonators have only low impedance sections for a better power handling.

References

[1] J.-S. Hong and M. J. Lancaster, "Couplings of microstrip square open-loop resonators for cross-coupled planar microwave filters," *IEEE Trans. Microwave Theory Tech.*, vol. 44, pp. 2099–2109, 1996.

[2] M. Sagawa, M. Makimoto, and S. Yamashita, "Geometrical structures and fundamental characteristics of microwave stepped-impedance resonators," *IEEE Trans. Microwave Theory Tech.*, vol. MTT-45, pp. 1078–1085, 1997.

[3] M. G. Banciu, R. Ramer, and A. Ioachim, "Microstrip filters using new compact resonators," *Electron. Lett.*, vol. 28, pp. 228–229, 2002.

[4] M. G. Banciu, E. Ambikairajah, and R. Ramer, "Microstrip filter design using FDTD and neural networks," *Microw. Opt. Technol. Lett.*, vol. 34, no. 3, pp. 219–224, 2002.

[5] F. S. Thomson, R. R. Mansour, S. Ye, and W. Jolley, "Current density and power handling of high-temperature superconductive thin film resonators and filters," *IEEE Trans. Appl. Supercond.*, vol. 8, no. 2, pp. 84–93, 1998.

[6] R. Levy, "Synthesis of general asymmetric singly- and doubly terminated cross-coupled filters," *IEEE Trans. Microwave Theory Tech.*, vol. 42, pp. 2468–2471, 1994.

[7] S. B. Cohn, "Dissipation loss in multiple-coupled-resonators filters," *Proc. IRE*, vol. 47, pp. 1342–1348, 1959.